Development of Integrated HEB/MMIC Receivers for Near-Range Terahertz Imaging

Fernando Rodriguez-Morales, *Student Member, IEEE*, K. Sigfrid Yngvesson, *Life Fellow, IEEE*, Richard Zannoni, Eyal Gerecht, *Member, IEEE*, Dazhen Gu, *Student Member, IEEE*, Xin Zhao, Niklas Wadefalk, and John J. Nicholson

***Abstract*—We present measurement results for a new type of integrated terahertz receiver, as an extension to previous work by the authors. The receiver we developed integrates quasi-optically coupled phonon-cooled NbN hot electron bolometric (HEB) mixers in close proximity with InP monolithic microwave integrated circuit (MMIC) intermediate-frequency (IF) amplifiers. We have measured antenna radiation pattern, receiver noise temperature, and bandwidth, as well as short-term stability of the integrated receivers. The measurements were performed at 1.6 and 2.5 THz over a very broadband IF frequency range. We have been able to extend the effective bandwidth of these receivers up to 5 GHz, the widest reported for any integrated configuration operating above 1 THz. The suitability of the HEB/MMIC approach for imaging applications has been confirmed through the development of a prototype system for near-range scanning. The results presented here are very promising for the future development of heterodyne focal plane arrays for space-based receivers, medical applications, and surveillance.**

***Index Terms*—Focal plane arrays, hot electron bolometric (HEB) mixers, imaging, integrated terahertz receivers, monolithic microwave integrated circit (MMIC) low-noise amplifiers (LNAs).**

I. Introduction

THE terahertz frequency range is loosely defined as the region of frequencies between 300 GHz and 3 THz. This part of the electromagnetic spectrum has traditionally found various important applications for high-resolution spectroscopy. These applications include earth, planetary, and space science. More recently, medical and surveillance imaging systems have been under development [1].

A number of coherent detector technologies has been developed over the past two decades to fulfill the requirements for low-noise receivers operating in the terahertz regime. Among these technologies we encounter Schottky diode mixers, superconducting-insulating-superconducting (SIS) junctions, and superconducting hot electron bolometric (HEB) mixers. Each of these technologies has inherent advantages and shortcomings. For example, Schottky diode mixers are inexpensive to fabricate and do not necessarily require operation in a cryogenic environment; however, they present a high local oscillator (LO) power consumption (on the order of 1 mW) and a limited noise performance. SIS mixers have a remarkable noise performance below 1.2 THz, but their sensitivity degrades very quickly beyond that frequency due to fundamental limitations. HEB mixers have the lowest noise performance for frequencies above 1 THz, in addition to having low LO power consumption (on the order of 1 μW), but the models that describe their behavior are yet to be completed. Still, HEB mixers represent the most promising technology for heterodyne detection beyond 1 THz.

In its most general configuration, a terahertz heterodyne receiver is composed of an active mixing element in cascade with a cryogenic low-noise amplifier (LNA) for the intermediate-frequency (IF) output. The available technologies for IF LNAs have evolved over time from GaAs field-effect transistors to high electron mobility transistors (HEMTs) [2], the current workhorse devices of the microwave/millimeter-wave world [3]–[5]. Moreover, advances in fabrication technologies and circuit modeling have made possible the advent of monolithic microwave integrated circuit (MMIC) LNAs. HEMT MMIC LNAs provide outstanding noise performance and very low dc-power consumption, with the additional advantage of reduced physical size [6]–[8].

In the aforementioned receiver configuration, the mixing element and the IF LNA (whether MMIC or not) are typically independent units connected by means of a coaxial transmission line. A cryogenic isolator is often added to the receiver chain in order to minimize standing waves between the mixer and the IF LNA and to guarantee the unconditional stability of the IF amplifier [Fig. 1(a)]. Currently available isolators occupy considerable physical space, increase the thermal load, and limit the receiver IF bandwidth to not more than an octave. The receiver arrangement as illustrated in Fig. 1(a) works well in most cases; in fact, several instruments designed for astrophysical observations are based on this configuration [9], [10]. Nevertheless, the development of terahertz heterodyne detectors has long called for receiver integration (and thus size reduction), a trend shared by most modern electronic circuits. Receiver miniaturization represents a significant advantage, especially for multiple receiver systems such as focal plane arrays (FPAs).

Significant progress has been made in this quest for compactness in submillimeter-wave receivers. One of the earliest conceptual arrays that suggested the use of terahertz detectors in close proximity with LNAs was described in [11]. The first integrated receiver based on an SIS junction and an HEMT IF

Manuscript received October 8, 2005; revised February 20, 2006. This work was supported by NASA through the Langley Research Center under Contract NAS1-01058 and by CONACyT, Mexico.

F. Rodriguez-Morales, K. S. Yngvesson, R. Zannoni, E. Gerecht, D. Gu, X. Zhao, and J. J. Nicholson are with the Department of Electrical and Computer Engineering, University of Massachusetts at Amherst, Amherst, MA 01002 USA.

N. Wadefalk was with the RF and Microwave Group, California Institute of Technology, Pasadena, CA 91125 USA. He is now with the Microwave Electronics Laboratory Group, Chalmers University of Technology, SE-412 96 Göteborg, Sweden.

Digital Object Identifier 10.1109/TMTT.2006.875257

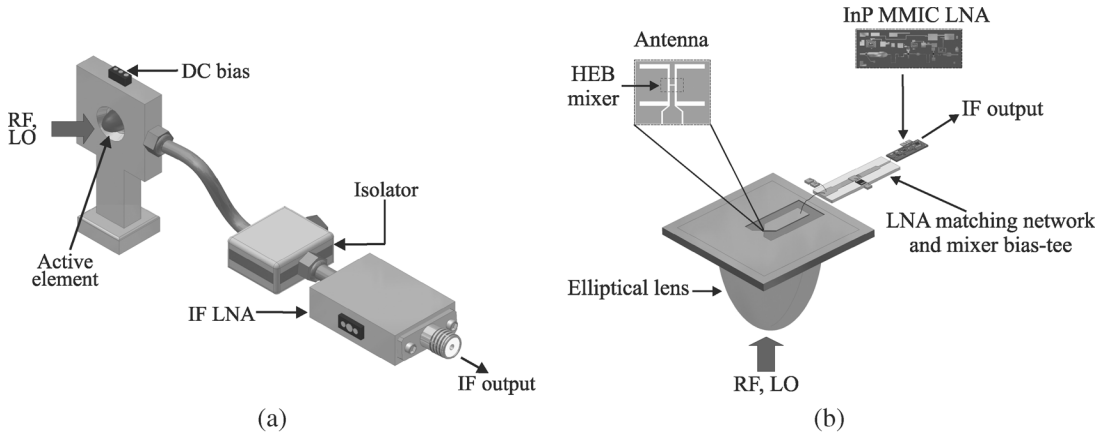

Fig. 1. Quasi-optical terahertz receivers: (a) traditional single-element receiver configuration and (b) integrated single-element receiver configuration.

amplifier was reported for 270 GHz in [12]. Later, a fully integrated array based on SIS mixers, superconducting quantum interference device (SQUID) IF amplifiers, and a superconducting Josephson-type LO was demonstrated at 500 GHz in [13]. The integration of HEB mixers and (GaAs) MMIC IF amplifiers was first proposed in [14], but it was not until several years later that such integration was actually implemented for a 1.6 THz focal plane array, using NbN HEBs and InP MMIC LNAs [15], [16].

In this paper, we extend [15] and [16] by presenting an extensive set of measurements performed on several NbN mixers, using the HEB/MMIC integrated approach. We have characterized antenna radiation pattern, optical coupling efficiency, receiver noise temperature, receiver IF bandwidth, and gain stability. Some of the measurements were performed for more than one local oscillator frequency. Furthermore, we describe the implementation of a prototype scanning system for near-range terahertz imaging. A similar imaging system has been recently reported for 640 GHz, using Schottky diode mixers [17]. The system we present operates at 1.6 THz and utilizes an HEB/MMIC receiver. The prototype is in the development stage and will undergo several improvements; however, preliminary results are in conformity with our design considerations.

This paper is organized as follows. Section II provides an overview of the design details for the integrated HEB/MMIC configuration. Section III describes the parameters measured and their importance for the optimum receiver operation. An outline of the laboratory setups and the experimental results are presented in Section IV. Section V discusses the implementation of the prototype scanning imager. A brief comparison of HEB/MMIC receivers with competing direct detectors is also given in Section V. Section VI addresses some considerations for the construction of large HEB/MMIC arrays, including issues pertaining to field deployment.

II. HEB/MMIC Receiver Overview

The configuration for the integrated receiver we have developed is shown in Fig. 1(b). The active mixer elements are phonon-cooled NbN HEB mixers fabricated on silicon substrates. The device chip size is 6 mm $\times$ 6 mm $\times$ 350 μm. Device dimensions are typically 4 μm wide by 0.5 μm long. The core of the HEB devices we use is the thin NbN superconducting film produced at Moscow State Pedagogical University, Moscow, Russia. The device fabrication was performed through collaboration with the National Institute of Standards and Technology at Boulder, CO, and Chalmers University of Technology, Göteborg, Sweden. The HEB mixers are integrated with planar twin-slot antennas or log-periodic antennas. Twin-slot antennas are narrow bandwidth and linearly polarized. Log-periodic antennas are broadband and the angle of polarization that yields the best response varies with frequency, depending upon the geometry of the teeth. The design center frequency of the two types of antennas we use throughout this paper is 1.6 THz. However, as will be shown, this technology can operate at significantly higher terahertz frequencies by properly scaling the antenna dimensions. We have chosen a quasi-optical scheme for radiation coupling, in which a 4-mm-diameter silicon elliptical lens is used in conjunction with the monolithic antenna.

The IF chain of the integrated receiver is composed of an InP MMIC LNA and additional microwave circuitry. The MMIC chips we use (size 0.75 $\times$ 2 mm) have been developed by Weinreb and Wadefalk at the Jet Propulsion Laboratory, California Institute of Technology [18], [19]. The chips were originally intended for use on the Allen telescope array [20]. These amplifiers have three 0.1 μm InP HEMT stages. They provide a high gain (up to 32 dB), remarkably low noise (less than 8 K over the band with a minimum of 3.5 K), and very broadband performance (0.5–11 GHz). An important feature of these chips is the possibility of adjusting the bias settings to minimize dc-power utilization. This adjustment can be made without significantly affecting the overall amplifier performance. The best noise conditions are obtained with 20 mW of power dissipation. The best tradeoff among sufficient gain, low power, and low-noise performance is achieved with only about 5 mW (Fig. 2). Low power consumption is particularly important for multipixel receiver systems.

In order to minimize the noise figure of the integrated receiver, the matching between the HEB mixer output and the MMIC input had to be optimized. This optimization required a knowledge of the HEB IF impedance as well as the optimal source impedance needed for the low-noise operation of the MMIC. The optimal source impedance of the amplifier was obtained using computer simulations and measurements. In

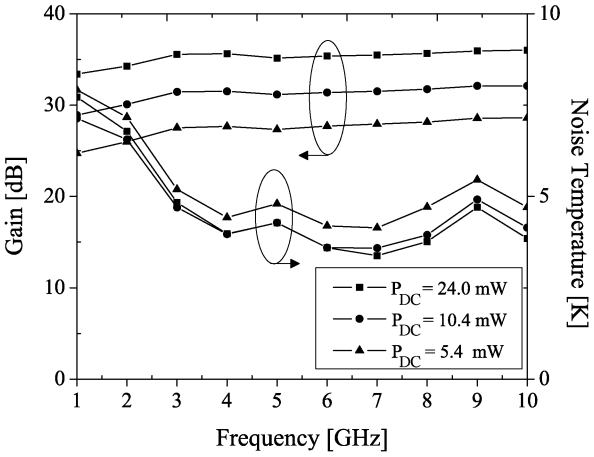

Fig. 2. Measured performance of the MMIC low-noise amplifier used in our receivers. A microstrip matching transformer was used at the input of the MMIC in order to yield minimum noise figure. The measurements were performed at an operating temperature of 11 K.

regards to the HEB mixer impedance, careful measurements have been carried out on custom-made NbN devices [16], [21]. These studies showed that the appropriate combination of LO power and dc bias leads to a mixer impedance dominated by the real part and close to the dc differential resistance dV/dI. The foregoing approximation holds for operating points near the optimum (lowest noise) and for frequencies below the IF noise bandwidth of the HEB mixer.[1] The imaginary part of the HEB impedance has been taken into account in our computer simulations as a small (though not negligible) reactance. With these considerations, it has been possible to accomplish a broadband coupling between the MMIC LNA and the HEB. This was achieved by employing a multisection microstrip matching transformer. This circuit provides a near-optimum reflection coefficient to the input of the MMIC while presenting an impedance close to 50 Ω as seen at the HEB terminals. Optimal noise operation of the MMIC is thus achieved when the dc differential resistance of the HEB is adjusted to be 50 Ω. However, dV/dI can be as high as 95 Ω at the optimum operating point for the mixer, in which case the noise temperature of the LNA will still be sufficiently low.

The microstrip matching transformer also eliminates the need for an isolator (which drastically reduces the size). All the required dc-bias networks are built on separate circuit boards and placed inside the integrated receiver module. The MMIC amplifier is enclosed in a narrow rectangular cavity in order to suppress undesired waveguide modes that could drive it into oscillation. The cavity is designed to have a cutoff frequency of 75 GHz, which is well above the maximum frequency of operation of the MMIC. A photograph of the HEB/MMIC integrated receiver is shown in Fig. 3. A simplified circuit diagram of the integrated receiver is shown in Fig. 4. C1 and L1 form a bias-tee with broadband performance for the HEB mixer.

[1]The IF noise bandwidth is defined as the frequency at which the receiver noise temperature doubles with respect to the low-frequency value. This parameter will be later denoted as B_N. A well-known feature of phonon-cooled HEBs is that B_N is typically (two times) wider than the conversion gain bandwidth [14].

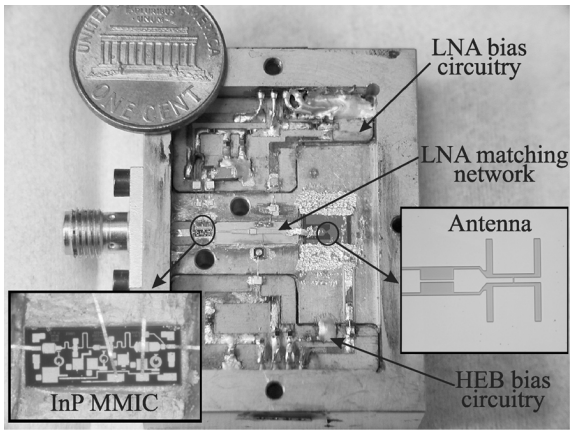

Fig. 3. Inside view of the integrated quasi-optical HEB/MMIC receiver. The antenna shown in this picture corresponds to a twin-slot design.

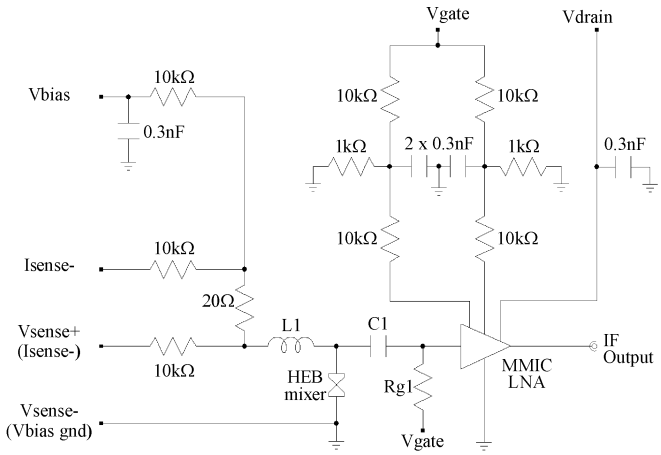

Fig. 4. Simplified circuit diagram of the integrated HEB/MMIC receiver. The MMIC LNA is biased with a common gate and a common drain voltage for all stages.

The integrated receiver is operated at 4 K, inside a liquid helium (LHe) cryostat. The LO source we use is a CO_2 laser-pumped far infrared (FIR) gaseous laser system. Although solid-state sources with sufficiently high power have become recently available [22]–[24], an FIR laser system is very well suited for extensive laboratory testing. Our system produces stable continuous-wave (CW) terahertz radiation with an output power up to about 100 mW. The LO laser can be readily tuned to different frequencies by changing the gas in the FIR tube. A mylar beam splitter with a thickness of 6 μm is used as diplexer between the LO and the signal beam. Two different LO laser frequencies are used for this paper: 1.63 and 2.5 THz. The 1.63 THz laser line runs on difluoromethane gas while the 2.5 THz line runs on methanol gas.

III. Receiver Characterization

As a first step for the validation of the HEB/MMIC approach, we conducted a variety of tests on different NbN mixer devices. A description of the different parameters that were measured and the relevance they have to this investigation is outlined next.

A. Antenna Radiation Pattern

For a linearly polarized antenna, performance is often described in terms of its principal E- and H-plane patterns [25]. The quality of the beam pattern is thus an important parameter to describe the performance of the integrated receiver from the quasi- optical point of view. The far-field pattern of the integrated antenna is primarily determined by the aperture of the elliptical lens [26]. Knowing the antenna radiation pattern profile is essential to achieve an efficient use of the focal plane space with which the antennas sample the incoming radiation [11]. The lens/antenna combination we use is capable of coupling over 90% of the radiation pattern to a single Gaussian mode [26].

B. Receiver Noise Temperature and Effective Bandwidth

The root mean square (rms) fluctuations in the measured radiation temperature of a coherent detector system are given by the basic radiometer formula

$$\Delta T_{\rm rms} = \frac{T_{\rm sys}}{\sqrt{B \cdot \tau}} + \left(\frac{\Delta G}{G}\right) T_{\rm sys} \tag{1}$$

where $T_{\rm sys}$ is the system noise temperature, B is the receiver bandwidth, τ is the integration time, and ΔG represents the change (rms) in the system gain G.[2] In order to achieve the maximum receiver sensitivity, $\Delta T_{\rm rms}$ needs to be minimized. Therefore, our integrated receiver system benefits from a large bandwidth and low noise temperature.

The bandwidth of the integrated receiver is thus an important parameter that needs to be defined. For this purpose, two important figures of merit are used: the IF noise bandwidth B_N and the effective receiver bandwidth $B_{\rm eff}$. Both figures of merit are closely related to the measured noise performance. B_N has been introduced in Section II and can be obtained by inspection from the experimental noise data. The use of B_N is most appropriate to estimate the bandwidth of astronomy receivers that detect narrow spectral lines within a given spectral window [29]. When using a terahertz receiver to detect broadband thermal radiation, though, it is best to use $B_{\rm eff}$ to quantify the usable bandwidth [$B = B_{\rm eff}$ in (1)]. The effective receiver bandwidth can be obtained based on the measured variation of the receiver noise temperature with IF frequency. We define $B_{\rm eff}$ by integrating the expression for the inverse of $\Delta T_{\rm rms}^2$ versus IF frequency

$$\frac{1}{\Delta T_{\rm rms}^2} = \int_{f_0}^{\infty} \frac{1}{T_{sys}^2(f)} df \cdot \tau = \frac{B_{\rm eff} \cdot \tau}{T_{\rm sys}^2(f = f_0)} \tag{2}$$

$$B_{\rm eff} = T_{\rm sys}^2(f = f_0) \cdot \int_{f_0}^{\infty} \frac{1}{T_{\rm sys}^2(f)} df \tag{3}$$

where f_0 is the lowest frequency at which the MMIC amplifier produces a low noise temperature (0.5 GHz in our case) and $T_{\rm sys}(f)$ is a polynomial fit to the measured noise temperature response.

[2]It is assumed that fluctuations in the receiver output due to gain variations are independent of the fluctuations resulting from system noise [27], [28].

C. Stability

Another parameter that can be adjusted in (1) to minimize $\Delta T_{\rm rms}$, is the integration time τ. Ideally, one would like to integrate for long periods of time ($\tau \to \infty$). However, τ cannot be made indefinitely large, lest the signal-to-noise ratio be reduced [30]. The upper limit for τ is constrained by the short-term gain stability of the system. Gain fluctuations determine the second term to $\Delta T_{\rm rms}$ in (1) and must be considered carefully in the design of a terahertz receiver system. A statistical parameter called *Allan variance* is a practical benchmark for assessing the contribution of different noise types and drift in system gain to the overall receiver stability. This parameter is a two-sample variance taken on the variable x. Each value of x in a set has been averaged over an interval τ, and the samples of x are taken in an adjacent series, namely, [31]

$$\sigma_A^2(\tau) = \frac{\langle (\Delta x)^2 \rangle}{2}. \tag{4}$$

In our case, the variable x is the instantaneous IF output power of the receiver. A log–log plot of the Allan variance versus integration time is commonly referred to as an *Allan plot*. According to (4), for the ideal case of having totally uncorrelated (Gaussian) noise, the Allan plot should be a straight line with a slope $1/\tau$. In a real sensitive receiver, however, this holds true only for sufficiently small values of τ ($\tau < T_A$). As the integration time increases, the contribution to the receiver output power made by the low frequency drift and $1/f$ noise becomes significant. This causes the Allan plot to diverge from the ideal behavior predicted by the first term in the radiometry equation. The Allan time T_A is thus defined as the largest possible integration time for which the $1/f$ noise and gain fluctuations can be neglected. For $\tau > T_A$, the integration efficiency is substantially reduced.

The $1/f$ regime in the Allan plot is characterized by a nearly constant variance. For times much longer than T_A, the slow drift in system gain starts to dominate and the Allan variance increases with integration time ($\sigma_A^2(\tau) \propto \tau$). When one compares the Allan times (T_A and T_A') measured at two different bandwidths (B and B'), the following relationship has been proposed [32]:

$$T_A / T_A' = (B/B')^{\frac{1}{\beta+1}}. \tag{5}$$

Here, β is a parameter that is one if $\sigma_A^2(\tau)$ transitions from being proportional to $1/\tau$ to a $1/f$ noise region and two if the transition is to $\sigma_A^2(\tau) \propto \tau$.

IV. Results and Discussion

The HEB devices under test were designated A–E. Mixers A, B, and E were integrated with log-periodic antennas. Devices C and D had twin-slot antennas. For each specimen, the corresponding elliptical lens was attached to the back of the device chip using purified bee's wax. The precise alignment between the antenna and the center of the lens was done manually under a high magnification optical microscope. Photolithographically patterned marks on the back of the mixer chip were used as a reference for the alignment. With this method we can achieve a device/lens registration accuracy of at least 100 μm [14].

A. Antenna Radiation Pattern

These measurements were completed at 1.6 THz and only for twin-slot antenna devices. Results for the log-periodic version have been reported in earlier work by Ji [33]. The HEBs were operated as direct detectors for these measurements. We required the use of a special fixture instead of the integrated mixer block. This is justified since the quasi-optical part of the receiver remained unchanged after the optical test. The operating temperature of the device under test was increased to 8 K (just below the critical temperature of the superconducting NbN film) using a power resistor heater. This step was done in order to achieve maximum sensitivity. The laser beam was used as an input source and scanned vertically (for the E-plane) and horizontally (for the H-plane). The output voltage (after preamplification) was continually recorded from a lock-in amplifier using its general-purpose interface bus (GPIB) port and a LabView program. To accomplish the beam scanning, we used a rotating mirror mounted on a special translation unit. The mirror steered the beam with small angular increments while keeping it focused in the aperture plane of the elliptical lens. The FIR beam was chopped by means of an acoustooptical modulator, placed at the output of the CO_2 laser beam. A chopping frequency of 100 Hz was used. The distance between the FIR beam and the antenna was about 1 m. Absorbing material was placed around the liquid helium dewar and nearby metallic surfaces to reduce unwanted beam reflections as much as possible.

Fig. 5 shows the antenna pattern for device D, obtained for both horizontal and vertical planes. The theoretical predictions were obtained using a ray-tracing/field-integration approach [26]. The full-width at half-maximum (FWHM) beamwidth was determined to be close to 3.5°, in agreement with design considerations. The asymmetry in the radiation pattern plots reflects a slight misalignment (off-axis mismatch) between the HEB device and the elliptical lens. The misalignment was estimated by using a data fitting method, in which two parameters (magnitude and angle of the off-axis mismatch) were adjusted to fit the experimental data to the numerical predictions. The magnitude component of the mismatch is measured from the center of the lens while the angular component is measured with respect to the horizontal plane (H-plane) of the antenna. The off-axis mismatch was thus found to be 94 μm at an angle of 13°. These fitting parameters are within the accuracy expected from our assembly method (100 μm). A global agreement between theoretical calculations and measured results has been obtained for all devices [34].

For a large imaging array, it is desirable to minimize the spacing between adjacent pixels in order to enhance the spatial resolution. Our measurements of the antenna pattern confirm that the optimum interelement spacing is close to the diameter of the lenses (4 mm in this case), as also demonstrated for a similar optical configuration in [13]. These results are also consistent with the optical coupling measurements reported in [15].

B. Receiver Noise Temperature and Effective Bandwidth

In order to obtain $T_{\rm sys}$, we measured the double-sideband noise temperature as a function of frequency for all devices. We used the standard Y-factor method, in which a hot/cold blackbody radiation source is inserted into the signal beam path, while the change in IF output power is recorded. We have a tunable IF back-end (with a 200 MHz bandwidth) that enables us to perform broadband noise measurements. All five HEB devices (A through E) were tested with the same block in order to perform direct comparisons. The twin-slot antenna devices were tested only at 1.6 THz. Devices A, B, and E were tested at both 1.6 and 2.5 THz. In all measurements, both the MMIC and the HEB under test were biased for lowest noise performance. The optimum dc operating conditions used for each device are summarized in Table I. The parameter I_c denotes the critical current of the superconducting film. The value of dV/dI was obtained from a polynomial fit to the I–V curve, evaluated at the optimum point.

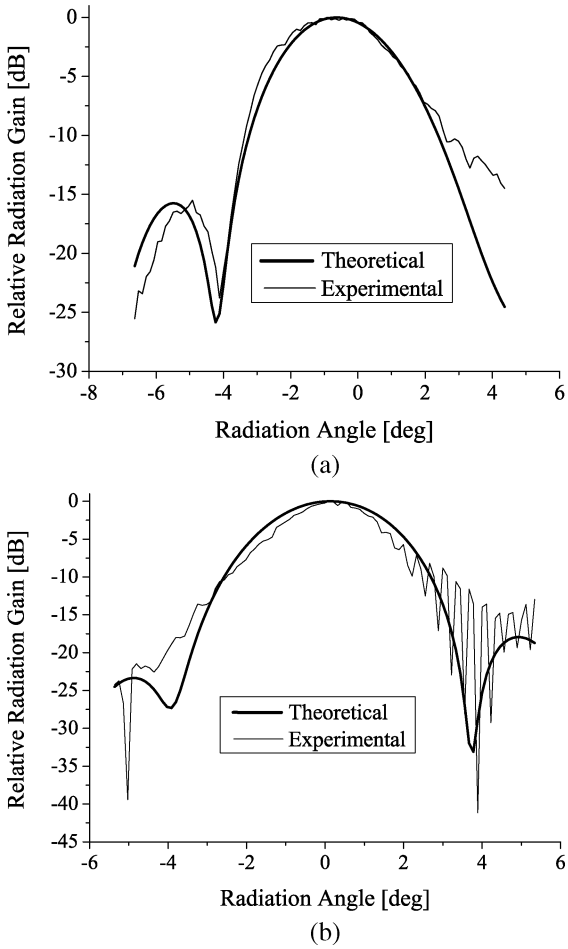

Fig. 5. Antenna radiation pattern for device D. (a) E-plane. (b) H-plane.

TABLE I
OPTIMUM DC OPERATING CONDITIONS*

Device #	I_c μA	V_0 mV	I_0 μA	R_0 Ω	dV/dI Ω
A	350	0.75	43	17.4	72
B	250	0.50	36	13.8	80
C	260	0.70	37	17.5	76
D	200	0.60	40	15.0	74
E	100	0.50	30	16.6	90

* LNA bias settings: $\mathrm{V}_d = 1.1$ V, $\mathrm{I}_d = 16$ mA.

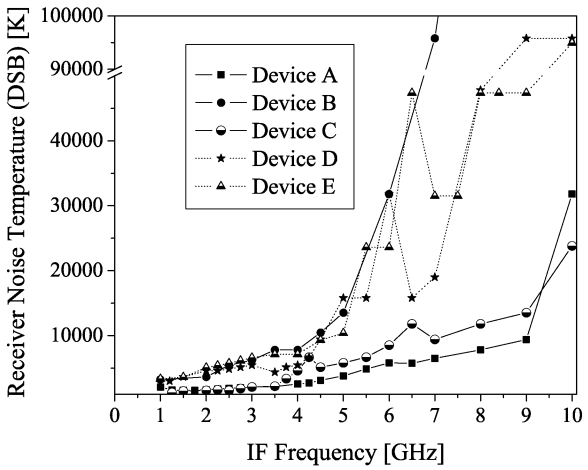

Fig. 6. Noise performance for different NbN devices measured at 1.6 THz using the HEB/MMIC approach.

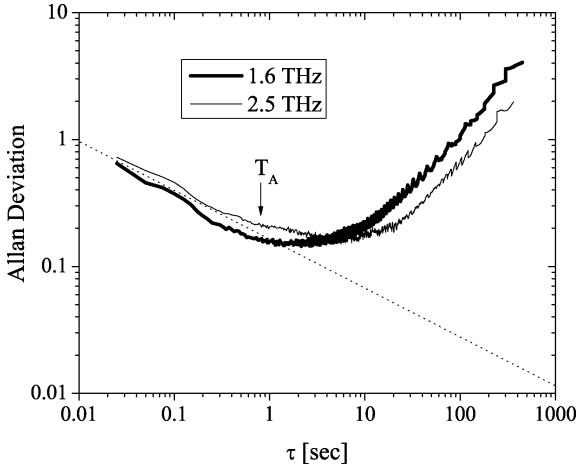

Fig. 7. Measured Allan deviation (square root of the Allan variance) for device B. The dotted line indicates the ideal response of the receiver (slope $1/\sqrt{\tau}$).

TABLE II
SUMMARIZED NOISE AND IF BANDWIDTH PERFORMANCE

Device #	NT (at 1.6 THz)	NT (at 2.5 THz)	B_N GHz	B_{eff} GHz
A	1600 K	2046 K	4.5	5.0
B	3200 K	5400 K	3.5	3.2
C	1200 K	N/A	3.4	2.9
D	3000 K	N/A	4.2	4.0
E	3500 K	5800 K	3.0	2.2

Fig. 6 shows the measured noise response for detectors A through E, all measured at 1.6 THz. We have deliberately included all responses in the same graph in order to point out the differences in performance. In the first place, one can see the dissimilarities in the magnitude of the noise temperature for low IF frequencies, which are in fact in agreement with our expectations. These discrepancies are mainly due to the unequal I–V characteristics of the HEB mixers [15].

A noticeable difference in the smoothness of the noise response for different devices is also apparent from Fig. 6. The dotted lines (devices D and E) indicate measurements in which some of the components of the receiver exhibited poor performance at high IF frequencies. In particular, the microwave properties of the bias resistor for the first HEMT's gate of the MMIC (Rg1 in Fig. 4) as well as the spiral inductor (L1) used in the integrated mixer bias-tee had a strong impact on the LNA noise temperature. A significant improvement was achieved for devices A, B, and C, for which we used components with higher self-resonant frequency. Thus, we conclude that the quality of the components used in the IF circuitry plays a major role in the performance of the integrated receiver.

Table II presents a summary of important results obtained for the devices measured in the integrated mixer block. The table includes the receiver double-sideband noise temperature (NT) measured at the lowest IF frequency (1 GHz), the IF noise bandwidth, and the effective bandwidth. The latter has been calculated through numerical integration, using (3). The HEB/MMIC combination using device A presents the best overall performance (low noise, widest bandwidth). This mixer was ultimately chosen to be used in the prototype imaging system that will be described in Section V.

In HEB/MMIC receivers, the effective bandwidth is predominantly constrained by a nontrivial interaction between the mixer and the LNA. Modeling this interaction both accurately and rigorously is a major challenge, mostly because currently available models for HEBs lack completeness [35]–[38]. Aggravating the matter, the noise parameters of the amplifier change when the source impedance is not equal to 50 Ω but instead equal to the IF output impedance of the phonon-cooled mixer [39]. Having achieved effective bandwidths of more than 4 GHz using standard model calculations is therefore a significant accomplishment.

Two variables that strongly influence the profile of the HEB impedance, and therefore the bandwidth of the receiver, are the electron temperature relaxation time τ_θ and the resistance change as a function of absorbed power dR/dP. τ_θ is a thermal time constant that is in itself a complicated function of other parameters such as the electron–phonon interaction time $\tau_{\mathrm{e-ph}}$, the ratio of the specific heats c_e/c_{ph}, the electron–electron interaction time τ_{e-e}, and the phonon escape time from the NbN film to the substrate τ_{esc} [40].

C. Stability

The Allan variance measurements were completed using the two LO laser lines indicated in Section II. The bias settings were adjusted for lowest noise operation. The IF output power was then continuously recorded using an Agilent E4418B power meter. An 80 MHz bandwidth (centered at 1.9 GHz) was used. The data were synchronously acquired from the instrument through its GPIB interface and processed by means of LabView software. Fig. 7 shows a plot of the Allan deviation (square root of the Allan variance) as a function of integration time τ for device B. Our measured value for the Allan time T_A is nearly 1 s for both 1.6 and 2.5 THz. Allan times measured for other devices were also in the order of 1 s, in agreement with the results reported by other research groups for HEB devices of comparable size [41], [42].

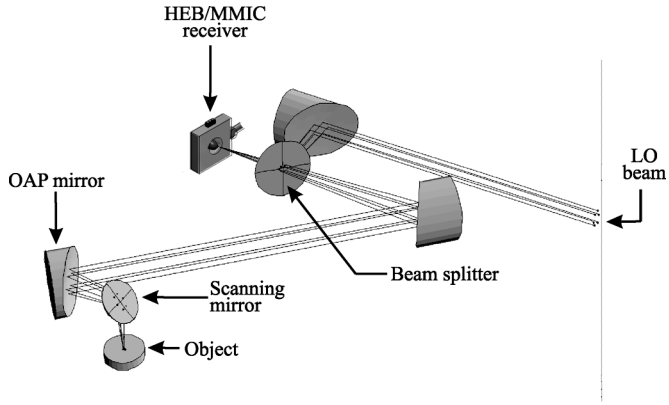

Fig. 8. Optical diagram for the prototype imager.

V. Imaging Using an Integrated HEB/MMIC Receiver

Imaging can be considered to be the process of measuring the radiation arriving from different directions [43]. Millimeter-wave imaging systems have so far been demonstrated at frequencies close to 100 GHz [44], [45]. These systems have primarily been coherent and employed HEMT amplifiers used as preamplifiers to ensure high sensitivity. A competing approach employs direct Nb detectors but requires active illumination to realize sufficient sensitivity [46]. For passive detection, as considered here, our terahertz system is about three orders of magnitude more sensitive. In order to compete with a heterodyne system, direct detectors would be required to also be cooled. A Nb detector cooled to 4.2 K with improved sensitivity was recently demonstrated in the laboratory [47]. No direct detector systems cooled to 4.2 K presently exist that can compete with our heterodyne system, though. We will present a brief quantitative performance evaluation in Section V-C to back up this claim.

Direct detector systems designed for use in astronomy can be more sensitive but require sub-kelvin cooling, which makes them impractical for most other applications. Even for astronomy, heterodyne detectors are superior in high-resolution spectroscopy applications [48]. In this paper, we desire to evaluate the new HEB detector array systems primarily for nonastronomy terahertz imaging applications. Examples of such systems include standoff security scanning systems and terahertz imaging systems used in biology and medicine [49]. Hence, we have developed a prototype system capable of scanning thermal radiation from a nearby laboratory target that uses the single element heterodyne mixer described earlier in this paper as detector. The system will be discussed in this section.

A. Description of the Prototype Imaging System

The system we developed utilizes an oscillating plane mirror as scanning reflector. The radiation emitted by the target is collected by this mirror and focused through two offset-axis paraboloid (OAP) mirrors onto the MMIC/HEB detector. The scanning mirror is located at about 5 cm from the target area. Fig. 8 shows the optical diagram for the prototype scanning system. The plane mirror rotates by approximately 30° at a rate of 8 Hz, driven by a standard electromagnetic actuator. The actuator is in turn excited by a triangle wave. The receiver IF output power level is further increased by a broadband amplifier operating at room temperature. A low-pass filter (LPF) with a cutoff frequency of 4 GHz is placed in cascade to limit the bandwidth to the effective bandwidth of the receiver as determined in Section IV-B. The output of the LPF is connected to a standard microwave detector in order to produce a rectified voltage. The detected signal is averaged and displayed on a digitizing oscilloscope. This technique allows us to obtain a linear image of one line in the target [50]. The system can in principle be extended to obtain two-dimensional imagery of an object. This can be achieved, for example, via controlled motion of the scan target in the direction perpendicular to the scanning plane.

B. Results

Using the method outlined in the previous section, we have recorded the image of a step from a room temperature load (280 K) to a liquid nitrogen $(\mathrm{LN_2})$ temperature load (77 K), as shown in Fig. 9(a). These measurements were performed at 1.6 THz using detector A (discussed in Section IV-B). The step was located approximately in the center of the scanned length. The measured noise temperature at the image was about 3000 K. The effective integration time on a pixel was 200 ms, which was obtained based on the scan rate and the size of the target. The image records a peak-to-peak level of 43 mV for a $\Delta\mathrm{T}$ of about 200 K. From this, a responsivity of 0.2 mV K^{-1} is inferred. Fig. 9(b) shows an image obtained in a similar fashion for a steel bar in thermal equilibrium with a THz absorber background. The absorber was cooled to a temperature (280 K)[3] slightly below that of the surroundings. The peak-to-peak level obtained in this case is 3 mV, which translates to a $\Delta\mathrm{T}$ of approximately 15 K. The steel bar is essentially a perfect reflector (>99%) of the ambient thermal radiation, which was at about 295 K. The 15 K signal obtained from the steel bar is consistent with these facts. The noise in this image is less than 0.3 mV rms. Hence, the fluctuation level at the system input is equivalent to a thermal signal of less than 1.5 K rms. This value is far greater than what would be expected from the radiometry formula, ignoring the contribution of gain fluctuations (0.1 K). Theory predicts that for white noise, the Allan time varies inversely proportional to the bandwidth, which could explain why ΔT_{rms} is larger than the first term in (1).[4] No measurements have been published that support this prediction for HEB receivers, however. Our own recent measurements actually show about the same Allan time for $B = 80$ MHz, 3 GHz, and 4 GHz. Moreover, for terrestrial terahertz imaging systems, a typical integration time per pixel may be about 10 ms, so the most important range in the Allan variance diagram is for such short times, well below the typical value for T_A in HEBs. We are presently performing additional Allan time measurements for different bandwidths and the results will be published in a future paper. Our results also show some effects due to 60 Hz, but these are traceable to the bias power supplies and will be eliminated as our system is further

[3]The temperature of the background absorber was measured using a calibrated thermometer.

[4]The Allan time of 1 s as obtained in Section IV-C was measured for a bandwidth of 80 MHz. However, our imaging system uses the effective bandwidth almost entirely (4 GHz).

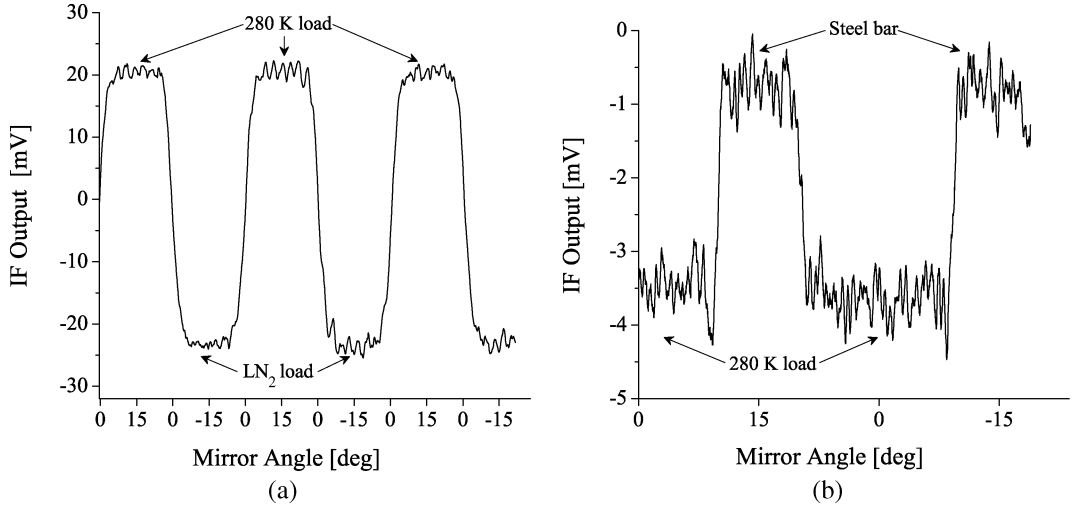

Fig. 9. Test recordings from the prototype line imager: (a) step from a load at 280 K to a LN_2 temperature load and (b) steel bar over a background consisting of a load at 280 K.

developed. In spite of the present limitations, the capability of this technology for obtaining imagery using scanning has been shown. We fully expect that we can reach the theoretical sensitivity predicted from the radiometer formula with our heterodyne detector arrays.

C. Comparison With Direct Detectors

We finally ask how the performance of the HEB/MMIC detectors compares with that of direct detector arrays. The sensitivity of direct detectors is characterized by their noise equivalent power (NEP) in units of $\mathrm{WHz}^{-1/2}$. The $\mathrm{Hz}^{-1/2}$ dependence arises from the postdetection bandwidth $= 1/2\tau$, where τ is the integration time that we used to evaluate the heterodyne detectors above. We can convert ΔT_{rms} for a heterodyne system, as given by (1), to NEP as follows:

$$\mathrm{NEP} = k_B \cdot \Delta T_{\mathrm{rms}} \cdot B \tag{6}$$

where k_B is Boltzmann's constant. For our prototype system, we find NEP $= 8 \times 10^{-14}$ $\mathrm{WHz}^{-1/2}$ while an optimized HEB detector system ($\Delta T_{\mathrm{rms}} = 16$ mK) could achieve NEP $= 10^{-15}$ $\mathrm{WHz}^{-1/2}$. The room-temperature direct detector system in [51] has an NEP of 5×10^{-11} $\mathrm{WHz}^{-1/2}$ and $\Delta T_{\mathrm{rms}} = 18$ K, compared with 16 mK for the optimized HEB heterodyne system, making heterodyne detector arrays three orders of magnitude more sensitive. The lowest NEP reached in a 4.2 K direct detector implemented in an imaging system so far is 2×10^{-12} $\mathrm{WHz}^{-1/2}$ [52]. This results in a $\Delta T_{\mathrm{rms}} = 720$ mK, assuming a 200 GHz bandwidth, roughly equivalent to a typical atmospheric absorption "window." The optimized heterodyne system is thus about a factor of 50 more sensitive at the present time. While direct detector systems may still improve, they are clearly not as well developed at terahertz frequencies as the heterodyne system we describe, which has already been demonstrated up to 2.5 THz. We also note that the 4.2 K direct detector system will require integrated SQUID amplifiers to achieve its optimum sensitivity. This fact cancels much of the attraction of room-temperature direct detectors derived from their simplicity in comparison with heterodyne systems.

VI. Considerations for Future HEB Arrays

A. Array Size

The desired characteristics of a terahertz imaging system for modern security applications impose certain specifications that need to be met. These requirements can be summarized as follows:

- spatial resolution of 1 cm across a 2 m $\times$ 1 m target at a distance of 25 m;
- temperature resolution of 1 K (rms);
- acquisition time of a full image compatible with video rates, in the range 30–100 ms.

These specifications are taken from DARPA solicitation BAA-04-07, "Terahertz Imaging Focal Plane Array Technology (TIFT)" issued in December 2003, and can be considered typical. With our presently available HEB/MMIC detectors, developing an array that provides the required spatial resolution would necessitate 2×10^4 elements. This number of pixels is beyond means and unfeasible to obtain at this stage. However, for future HEB array development, it would be possible to meet the above requirements by using a combination of scanning and a focal plane array with a reduced number of detectors. To accomplish the required temperature resolution of 1 K using a receiver with $NT = 1200$ K and $B_{\mathrm{eff}} = 5$ GHz, for example, the radiometer equation gives an integration time of 288 μs. For a frame rate of 60 ms, it is possible to produce $6 \times 10^{-2}/2.88 \times 10^{-4} = 208$ images by raster scanning. In order to produce a total of 2×10^4 pixels, the array needs to have $2 \times 10^4/208 \sim 96$ elements. A square FPA with 100 (10 $\times$ 10) elements will produce the required $\Delta T_{\mathrm{rms}} = 1$ K with some margin for downtime during scanning operations. The cross-sectional size of the square array will be very compact, about 6.5 cm by the side, considering that each element occupies an area of 6.5 mm $\times$ 6.5 mm. The required array can be

reduced to a smaller size linear configuration with scanning if the total target area is decreased and/or the special resolution (or frame time) requirements are relaxed. For security applications, a better tradoff between small array size and sufficiently small $\Delta T_{\rm rms}$ is expected for frequencies slightly lower than 1 THz, considering that the attenuation of typical clothing materials is lower in that region of the spectrum [53].

B. Cooling and Field Operation

At the moment, terahertz HEB receivers are all operated in cryogenic dewars that must be refilled with liquid helium about once every 24 h (see, for example, [9]). This is appropriate for astronomical receivers, but HEB receiver systems for other applications need to be integrated in a closed-cycle refrigerator system. There are refrigerator systems available for laboratory use from several companies. These are still bulky and require large amounts of electrical power and often cooling water for the compressor unit, but could be used in medical/biological imaging applications, for example. A portable terahertz camera can potentially be developed based on cooling systems under development for space applications [54], [55]. Such coolers would need extensive (and expensive) further development in order to minimize power consumption, size, and weight for a portable application. Nonetheless, they could be realized if a sufficiently attractive application arises.

VII. Conclusion

A new type of integrated receiver for terahertz frequencies based on NbN HEB mixers and InP MMIC IF amplifiers has been presented and extensively characterized. Measurement results are reported for 1.6 and 2.5 THz over a very broadband IF frequency range. The noise performance of the integrated receivers is in the range of 10–20$\times hf/k$. Effective receiver bandwidths up to 5 GHz can be achieved using this technology. The integrated quasi-optical detectors provide an important advantage for multiple receiver systems such as focal plane arrays. In fact, a prototype FPA that makes use of this type of integrated detectors has been previously demonstrated [15]. We have also presented a prototype imaging system that utilizes an HEB/MMIC receiver. At this stage, the features of the imaging system are limited. However, the capability for producing images through scanning has been demonstrated. The imaging system is undergoing several improvements while a more complete system, also based on HEB/MMIC detectors, is being built. It is expected that presently available solid-state LO sources will help further reduce the overall system size. Potential uses for the HEB/MMIC receivers range from astrophysics to medical diagnostics and surveillance.

Acknowledgment

Grateful acknowledgement is made to Dr. S. Weinreb, Jet Propulsion Laboratory, Pasadena, CA, for supplying the MMIC chips as well as Dr. P. Khosropanah, Chalmers University of Technology, Göteborg, Sweden, for device fabrication. The authors are also grateful to V. Fath, University of Massachusetts at Amherst, for his help on the receiver block assembly.

References

[1] P. H. Siegel, "Terahertz technology," *IEEE Trans. Microw. Theory Tech.*, vol. 50, no. 3, pp. 910–928, Mar. 2002.

[2] T. Mimura, "The early history of the high electron mobility transistor (HEMT)," *IEEE Trans. Microw. Theory Tech.*, vol. 50, no. 3, pp. 780–782, Mar. 2002.

[3] M. Pospieszalski and E. Wollack, "Ultra-low-noise, InP field effect transistor radio astronomy receivers: State-of-the-art," in *Proc. 13th Int. Conf. Microw.s, Radar Wireless Commun (MIKON-2000)*, May 2000, vol. 3, pp. 23–32.

[4] N. Wadefalk, A. Mellberg, I. Angelov, M. Barsky, S. Bui, E. Choumas, R. Grundbacher, E. Kollberg, R. Lai, N. Rorsman, P. Starski, J. Stenarson, D. Streit, and H. Zirath, "Cryogenic wide-band ultra-low-noise IF amplifiers operating at ultra-low dc power," *IEEE Trans. Microw. Theory Tech.*, vol. 50, no. 6, pp. 1705–1711, Jun. 2003.

[5] A. Tessmann, "220-GHz metamorphic HEMT amplifier MMICs for high-resolution imaging applications," *IEEE J. Solid-State Circuits*, vol. 40, no. 10, pp. 2070–2076, Oct. 2005.

[6] S. Weinreb, R. Lai, N. Erickson, T. Gaier, and J. Wielgus, "W-band InP wideband MMIC LNA with 30 K noise temperature," in *IEEE MTT-S Int. Microw. Symp. Dig.*, 1999, vol. 1, pp. 101–104.

[7] J. Hacker, J. Bergman, G. Nagy, G. Sullivan, C. Kadow, H. Lin, A. Gossard, M. Rodwell, and B. Brar, "An ultra-low power InAs/AlSb HEMT Ka-band low-noise amplifier," *IEEE Microw. Compon. Lett.*, vol. 14, no. 4, pp. 156–158, Apr. 2004.

[8] D. Dawson, L. Samoska, A. Fung, K. Lee, R. L. R. G. P. Liu, and R. Raja, "Beyond G-band: A 235 GHz InP MMIC amplifier," *IEEE Microw. Compon. Lett.*, vol. 15, no. 12, pp. 874–876, Dec. 2005.

[9] E. Gerecht, S. Yngvesson, J. Nicholson, Y. Zhuang, F. Rodriguez-Morales, X. Zhao, D. Gu, R. Zannoni, M. Coulombe, J. Dickinson, T. Goyette, W. Gorveatt, J. Waldman, P. Khosropanah, C. Groppi, A. Hedden, D. Golish, C. Walker, J. Kooi, R. Chamberlin, A. Stark, C. Martin, R. Stupak, N. Tothill, and A. Lane, "Deployment of TREND—A low noise receiver user instrument at 1.25 THz to 1.5 THz for AST/RO at the South Pole," in *Proc. 14th Int. Space Terahertz Technol. Symp.*, Tucson, AZ, Apr. 2003, pp. 179–188.

[10] S. Cherednichenko, M. Kroug, H. Merkel, P. Khosropanah, A. Adam, E. Kollberg, D. Loudkov, G. Goltsman, B. Voronov, H. Richter, and H.-W. Huebers, "1.6 THz heterodyne receiver for the far infrared space telescope," *Phys. C*, vol. 372–376, pp. 427–431, 2002.

[11] T. H. Buttgenbach, "An improved solution for integrated array optics in quasi-optical mm and submm receiver: The hybrid antenna," *IEEE Trans. Microw. Theory Tech.*, vol. 41, no. 10, pp. 1750–1760, Oct. 1993.

[12] S. Padin, D. Woody, J. A. Stern, H. LeDuc, R. Blundell, C. Tong, and M. Pospieszalski, "An integrated SIS mixer and HEMT IF amplifier," *IEEE Trans. Microw. Theory Tech.*, vol. 44, no. 6, pp. 987–990, Jun. 1996.

[13] V. P. Koshelets and S. V. Shitov, "Integrated superconducting receivers," *Supercond. Sci. Technol.*, vol. 13, pp. R53–R69, 2000.

[14] E. Gerecht, C. Musante, Y. Zhuang, K. Yngvesson, T. Goyette, J. Dickinson, J. Waldman, P. Yagoubov, G. Gol'tsman, B. Voronov, and E. Gershenzon, "NbN hot electron bolometric mixers, a new technology for low-noise THz receivers," *IEEE Trans. Microw. Theory Tech.*, vol. 47, no. 12, pp. 2519–2527, Dec. 1999.

[15] F. Rodriguez-Morales, K. S. Yngvesson, E. Gerecht, N. Wadefalk, J. Nicholson, D. Gu, X. Zhao, T. Goyette, and J. Waldman, "A terahertz focal plane array using HEB superconducting mixers and MMIC IF amplifiers," *IEEE Microw. Compon. Lett.*, vol. 15, no. 4, pp. 199–201, Apr. 2005.

[16] F. Rodriguez-Morales and K. Yngvesson, "Integrated THz receivers based on NbN HEB mixers and InP MMIC IF amplifiers," in *IEEE MTT-S Int. Microw. Symp. Dig.*, 2005, pp. 435–438.

[17] R. Dengler, A. Skalare, and P. Siegel, "Passive and active imaging of humans for contraband detection at 640 GHz," in *IEEE MTT-S Int. Microw. Symp. Dig.*, Jun. 2004, vol. 3, pp. 1591–1594.

[18] S. Weinreb and N. Wadefalk, 2005, private communication.

[19] N. Wadefalk and S. Weinreb, "Very low noise amplifiers for very large arrays," presented at the IEEE MTT-S Int. Microw. Symp./Very Large Microw. Arrays Radio Astron. Space Commun. Workshop, Long Beach, CA, Jun. 2005.

[20] D. DeBoer and D.-J. Bock, "The Allen telescope array: Splitting the aperture," *IEEE Micro*, vol. 5, pp. 46–53, Jun. 2004.

[21] F. Rodriguez-Morales and K. Yngvesson, "Impedance and bandwidth characterization of NbN hot electron bolometric mixers," in *Proc. 14th Int. Symp. Space Terahertz Tech.*, Tucson, AZ, Apr. 2003, pp. 431–438.

[22] A. Maestrini, J. Ward, H. Javadi, E. Schlecht, G. Chattopadhyay, F. Maiwald, N. Erickson, and I. Mehdi, "A 1.7–1.9 THz local oscillator source," *IEEE Microw. Compon. Lett.*, vol. 14, no. 6, pp. 253–255, Jun. 2004.
[23] J. Hesler, D. Porterfield, W. Bishop, T. Crowe, A. Baryshev, R. Hesper, and J. Baselmans, "Development and characterization of an easy-to-use THz source," in *Proc. 16th Int. Space Terahertz Technol. Symp.*, Göteborg, Sweden, May 2005, pp. 378–381.
[24] A. Maestrini, J. Ward, H. Javadi, C. Tripon-Canseliet, J. Gill, G. Chattopadhyay, E. Schlecht, and I. Mehdi, "Local oscillator chain for 1.55 to 1.75 THz with 100-μW peak power," *IEEE Microw. Compon. Lett.*, vol. 15, no. 12, pp. 871–873, Dec. 2005.
[25] C. Balanis, *Antenna Theory: Analysis and Design*. New York: Wiley, 1997.
[26] D. F. Filipovic, S. S. Gearhart, and G. M. Rebeiz, "Double-slot antennas on extended hemispherical and elliptical silicon dielectric lenses," *IEEE Trans. Microw. Theory Tech.*, vol. 41, no. 10, pp. 1738–1749, Oct. 1993.
[27] J. D. Krauss, *Radio Astronomy*. Powell, OH: Cygnus-Quasar Books, 1986.
[28] F. T. Ulaby, R. K. Moore, and A. K. Fung, *Microwave Remote Sensing: Active and Passive, Vol. I—Microwave Remote Sensing Fundamentals and Radiometry*. Reading, MA: Addison-Wesley, 1981.
[29] T. de Graauw, E. Caux, R. Gusten, W. Jellema, W. Luinge, J. Pearson, T. Phillips, R. Schieder, J. Stutzki, K. Wafelbakker, N. Whybom, and K. Wildeman, "The Herschel-Heterodyne Instrument for the far-infrared (HIFI)," in *Proc. Joint 29th Int. Conf. IR MM Waves 12th Int. Conf. Terahertz Electron.*, 2004, pp. 579–580.
[30] J. Kooi, G. Chattopadhyay, M. Thielman, T. Phillips, and R. Schieder, "Noise stability of SIS receivers," *Int. J. Infrared Millim. Waves*, vol. 21, no. 5, pp. 698–716, May 2000.
[31] D. Allan, "Should the classical variance be used as a basic measure in standards metrology?," *IEEE Trans. Instrum. Meas.*, vol. IM-36, no. 3, pp. 646–654, Jun. 1987.
[32] J. Kooi, J. Baselmans, A. Baryshev, R. S. M. Hajenius, J. Gao, T. Klapwijk, B. Voronov, and G. Gol'tsman, "Stability of heterodyne terahertz receivers," *J. Appl. Phys.*, 2005, submitted for publication.
[33] M. Ji, "Lens coupled printed antenna characterization," M.S. thesis, Univ. Massachusetts at Amherst, Amherst, MA, 2001.
[34] X. Zhao, "Integrated antennas for THz hot electron bolometer mixers," M.S. thesis, Univ. Massachusetts at Amherst, Amherst, MA, 2005.
[35] H. Ekstroem, B. Karasik, E. Kollberg, and K. Yngvesson, "Conversion gain and noise of niobium superconducting hot-electron mixers," *IEEE Trans. Microw. Theory Tech.*, vol. 43, no. 4, pp. 938–947, Apr. 1995.
[36] M. Kroug, "NbN hot electron bolometer mixers for a quasi-optical THz receiver," Ph.D. dissertation, Chalmers Univ. Technol., Göteborg, Sweden, 2001.
[37] H. Merkel, P. Khosropanah, P. Yagoubov, and E. Kollberg, "A hot-spot mixer model for phonon-cooled NbN hot electron bolometric mixers," *IEEE Trans. Appl. Superconduct.*, vol. 9, no. 6, pp. 4201–4204, Jun. 1999.
[38] H. Merkel, P. Khosropanah, S. Yngvesson, S. Cherednichenko, M. Kroug, A. Adam, and E. Kollberg, "An active zone small signal model for hot electron bolometric mixers," in *Proc. 12th Int. Space Terahertz Technol. Symp.*, San Diego, CA, Feb. 2001, pp. 67–74.
[39] R. Hu and S. Weinreb, "A novel wide-band noise parameter measurement method and its cryogenic application," *IEEE Trans. Microw. Theory Tech.*, vol. 52, no. 5, pp. 1498–1507, May 2004.
[40] S. Cherednichenko, M. Kroug, H. Merkel, E. Kollberg, K. Yngvesson, B. Voronov, and G. Gol'tsman, "IF bandwidth of phonon cooled HEB mixers made from NbN films on MgO substrates," in *Proc. 11th Int. Space Terahertz Technol. Symp.*, Ann Arbor, MI, May 2000, pp. 219–227.
[41] T. Berg, S. Cherednichenko, V. Drakinskiy, H. Merkel, E. Kollberg, and J. Kooi, "Stability measurements of NbN HEB receiver at THz frequencies," in *Proc. 15th Int. Symp. Space Terahertz Technol.*, Northampton, MA, Apr. 2004, pp. 25–32.
[42] J. Baselmans, M. Hajenius, J. Gao, A. Baryshev, J. Kooi, T. Klapwijk, B. Voronov, P. deKorte, and G. Gol'tsman, "NbN hot electron bolometer mixers: Sensitivity, LO power, direct detection and stability," *IEEE Trans. Appl. Superconduct.*, vol. 15, no. 6, pp. 485–489, Jun. 2005.
[43] P. Goldsmith, C.-T. Hsieh, G. Huguenin, J. Kapitzky, and E. Moore, "Focal plane imaging systems for millimeter wavelengths," *IEEE Trans. Microw. Theory Tech.*, vol. 41, no. 10, pp. 1664–1675, Oct. 1993.
[44] D. C. W. Lo, L. Yujiri, G. Dow, T. Ton, M. Mussetto, and B. Allen, "A W-band direct-detection radiometric imaging array," in *IEEE 1994 Microw. MM-Wave Monolithic Circuits Symp.*, 1994, pp. 41–44.
[45] L. Yujiri, M. Shoucri, and P. Moffa, "Passive millimeter wave imaging," *IEEE Micro*, vol. 4, no. 3, pp. 39–50, Sep. 2003.
[46] E. N. Grossman, A. Luukanen, and A. J. Miller, "Terahertz active direct detection imagers," in *Proc. SPIE* , 2004, vol. 5411, pp. 68–77.
[47] A. Luukanen and J. P. Pekola, "A superconducting antenna-coupled hot-spot microbolometer," *Appl. Phys. Lett.*, vol. 82, pp. 3970–3972, Jun. 2003.
[48] J. Stutzki, U. Graf, C. Honingh, K. Jacobs, R. Schieder, and Siebertz, "Terahertz receivers for astronomy," in *Proc. Joint 30th Int. Conf. IR MM Waves 13th Int. Conf. Terahertz Electron.*, Sep. 2005, vol. 2, pp. 403–404.
[49] P. H. Siegel, "Terahertz technology in biology and medicine," *IEEE Trans. Microw. Theory Tech.*, vol. 52, no. 10, pp. 2438–2447, Oct. 2004.
[50] R. Zannoni, S. Yngvesson, F. Rodriguez-Morales, J. Nicholson, D. Gu, and E. Gerecht, "A prototype terrestrial terahertz imaging system," in *Proc. 16th Int. Symp. Space Terahertz Tech.*, Göteborg, Sweden, pp. 93–97.
[51] A. Luukanen, A. J. Miller, and E. N. Grossman, "Active millimeter-wave video rate imaging with staring 120-element microbolometer array," *Proc. SPIE*, vol. 5411, pp. 195–201, 2004.
[52] ——, "Passive hyperspectral terahertz imagery for security screening using a cryogenic microbolometer," *Proc. SPIE*, vol. 5789, pp. 125–134, 2004.
[53] J. E. Bjarnason, T. L. J. Chan, A. W. M. Lee, M. A. Celis, and E. R. Brown, "Millimeter-wave, terahertz, and mid-infrared transmission through common clothing," *Appl. Phys. Lett.*, vol. 85, no. 4, pp. 519–521, Jul. 2004.
[54] D. Glaister, W. Gully, R. Ross, R. Stack, and E. Marquardt, "Ball aerospace 4–10 K space cryocoolers," *Proc. SPIE*, vol. 5498, pp. 768–774, Oct. 2004.
[55] R. Ross, *Cryocoolers 13*. Berlin, Germany: Springer-Verlag, 2005.

Fernando Rodriguez-Morales (S'00) received the B.S. degree in electronics engineering *(cum laude)* from Universidad Autónoma Metropolitana, México, in 1999, the M.Sc. degree in electrical and computer engineering from the University of Massachusetts at Amherst, in 2003, and is currently working toward the Ph.D. degree at the University of Massachusetts at Amherst.

From 2000 to 2001, he was with the Department of Physics and Astronomy, University of Massachusetts at Amherst, where he collaborated in the development of single electron transistor devices as well as semiconductor bolometer arrays. His research interests include the development of highly integrated HEB focal plane arrays for terahertz frequencies, as well as microwave and millimeter-wave circuit design and characterization.

K. Sigfrid Yngvesson (M'62–SM'92–F'98–LF'02) was born in Lidkoping, Sweden, in 1936. He received the Civilingenjor, Tekn.Lic., and Tekn.Dr. degrees in electrical engineering from Chalmers University of Technology, Göteborg, Sweden, in 1958, 1965, and 1968, respectively.

He was a Postdoctoral Fellow with the Department of Physics, University of California, Berkeley, in the 1960s. He has been with the Department of Electrical and Computer Engineering, University of Massachusetts at Amherst, since 1970, where he became a full Professor in 1978. He has worked on quantum electronic low-noise receivers for radio astronomy and on integrated arrays of antenna elements and active devices with applications to imaging and power combining. His present main research interests are in the areas of quasi-optical terahertz low-noise devices and applications. He is the author of *Microwave Semiconductor Devices* (Kluwer, 1991).

Richard Zannoni received the B.S. degree in electrical engineering and mathematics from the University of Massachusetts at Amherst, in 2004, where he is currently working toward the M.S. degree in electrical engineering.

His current research focuses on improving hot electron bolometer systems for high-speed imaging.

Eyal Gerecht (S'88–M'97) received the B.S.E.E. degree in electrical engineering with a minor in solid-state physics *(magna cum laude)* from the University of Houston, Houston, TX, in 1990, and the M.S.E.C.E. and Ph.D. degrees in electrical and computer engineering from the University of Massachusetts at Amherst, in 1994 and 1998, respectively.

In 1998, he joined the Department of Physics and Astronomy, University of Massachusetts at Amherst, as a Senior Postdoctoral Research Associate. Since 2000, he has been a Physicist with the Electromagnetic Division, National Institute of Standards and Technology, Boulder, CO, developing a number of terahertz-related technologies. His interests also include the development of receivers for millimeter and submillimeter applications.

Dr. Gerecht is a member of Tau Beta Pi and Eta Kappa Nu.

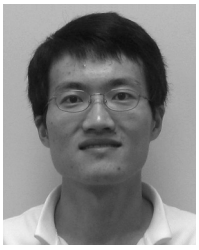

Dazhen Gu (S'01) received the B.S. degree in physics from Nanjing University, Nanjing, China, in 1999 and the M.S. degree in electrical engineering from the University of Massachusetts at Amherst, in 2004, where he is currently working toward the Ph.D. degree in electrical engineering.

From 1999 to 2001, he was a Research Assistant with the Superconductor Electronics Laboratory, Nanjing University, where he worked on the three-terminal device employing high Tc superconductor, ferroelectric, and ferromagnetic materials. Since 2001, he has been involved in the design and fabrication of NbN hot electron bolometric mixers for terahertz receivers. Since November 2003, he has been with the Electromagnetics Division, National Institute of Standards and Technology, Boulder, CO, where he is engaged in the development of terahertz imaging systems and characterization of low-noise amplifiers. His research interest includes nanofabrication, quantum electronics, and RF circuit design.

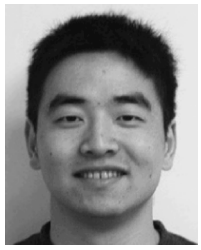

Xin Zhao received the B.S. degree in physics from the University of Science and Technology, China, in 2000, and the M.S. degree in electrical and computer engineering from the University of Massachusetts at Amherst, in 2005.

From 2002 to 2005, he was a Graduate Research Assistant with the Terahertz Laboratory, University of Massachusetts at Amherst, where his work focused on antenna design and numerical electromagnetic analysis and simulations, as well as measurements in the terahertz frequency range. Since 2005, he has been with Mathworks Inc, Natick, MA, developing hardware connectivity and data analysis software for test and measurement applications.

Niklas Wadefalk was born in Göteborg, Sweden, on May 14, 1973. He received the B.Sc. degree in electrical engineering from the Chalmers University of Technology, Göteborg, Sweden, in 1994.

Since 1995, he has been with the Microwave Electronics Laboratory Group, Chalmers University of Technology, except from 2001 to 2005, when he was with the RF and Microwave Group, California Institute of Technology, Pasadena, where he developed cryogenic MMIC amplifiers for various projects in the radio astronomy field such as the Allen Telescope array. His current research interests are broadband MMIC LNAs, microwave differential amplifiers, FET characterization, and noise-measurement techniques.

John J. Nicholson received the B.S. degree in marine biology and the associate degree in industrial technology/electronics and engineering science from Southeastern Massachusetts University of North Dartmouth (presently University of Massachusetts at Amherst) in 1976, 1984, and 1989, respectively.

From 1987 to 1996, he was with Millitech Corporation working on millimeter-wave and submillimeter-wave whisker contacted multipliers before becoming a semiconductor process engineer. He continued this work at Millivision, LLC, and became Lab Manager of the semiconductor fabrication facility. He joined the TREND group as a Research Engineer for the Department of Electrical and Computer Engineering, University of Massachusetts at Amherst, in May 2001, where he is also a Lab Instructor for the semiconductor fabrication course.